EARTH SURFACE PROCESSES AND LANDFORMS
Earth Surf. Process. Landforms **34**, 1533–1546 (2009)

Published online 1 July 2009 in Wiley InterScience
(www.interscience.wiley.com) DOI: 10.1002/esp.1845

Berm formation and dynamics on a gently sloping beach; the effect of water level and swash overtopping

Stine G. Jensen,[1]* Troels Aagaard,[1] Tom E. Baldock,[2] Aart Kroon[1] and Michael Hughes[3]
[1] Department of Geography and Geology, University of Copenhagen, Copenhagen, Denmark
[2] Division of Civil Engineering, The University of Queensland, St Lucia, Brisbane, Australia
[3] Marine & Coastal Environment Group, Geoscience Australia, Canberra, Australia

Received 4 October 2008; Revised 2 April 2009; Accepted 11 May 2009

* Correspondence to: S. G. Jensen, Department of Geography and Geology, University of Copenhagen, Øster Voldgade 10, DK-1350 Copenhagen K, Denmark.
E-mail: sgj@geo.ku.dk

ESPL
Earth Surface Processes and Landforms

ABSTRACT: Berm formation and morphological development of the beach face have been observed during a neap–neap tidal cycle on the gently sloping and accreting beach at Vejers, Denmark. During the field campaign, an intertidal bar migrated onshore and stabilized as a berm on the foreshore. A new intertidal bar occurred on the lower beach face, migrated onshore on the rising tide and finally merged with the pre-existing berm. As the tide continued to rise, the new berm translated further onshore as an intertidal bar to the uppermost part of the foreshore. The sediment transport during the berm transition was onshore directed in the upper swash and offshore directed in the lower swash. This berm development can be described through both the neap-berm, ridge-and-runnel and berm-ridge development concepts proposed by Hine (*Sedimentology* 1979; 26: 333–351), and all three stages were observed during only three tidal cycles. The main factors controlling this fast transformation were the gentle slope of the cross-shore profile, rapid water level translation rates, substantial swash overtopping of the berm, and low infiltration rates. Despite the onshore migration of intertidal bars and berm formation, no net foreshore accretion took place during the field campaign. This was largely due to the formation of rip channels with strong rip currents cutting through the intertidal bars and the berm, which acted as a sediment drain in the profile. Copyright © 2009 John Wiley & Sons, Ltd.

KEYWORDS: berm development; foreshore processes; morphodynamics; beach slope; swash overtopping

Introduction

Processes accounting for beach erosion have been widely studied and are relatively well-described in the literature. Based on these studies and descriptions, numerical models have been developed and are used extensively to compute beach erosion, even though most of the models exclude swash processes and hence cannot account for beach face accretion (Masselink and Puleo, 2006; Brocchini and Baldock, 2008). The main reason for this omission is the fact that the net sediment transport processes in the swash zone are poorly understood, despite advances in the overall understanding of gross sediment transport (Masselink and Hughes, 1998; Butt and Russell, 2000; Puleo *et al*., 2000; Pritchard and Hogg, 2005; Aagaard and Hughes, 2006). None the less, processes dominating shoreline accretion are essential for beach recovery, e.g. after a storm event. Being able to understand and describe these processes will not only contribute greatly to the understanding of beach behaviour but also improve existing models of shoreline development.

In order for a beach to accrete, a sediment input, either transported landwards through the swash zone to the upper beach face or, more locally, resulting from negative longshore transport gradients in the swash zone, is required. It is generally recognized that under high-energy conditions, the cross-shore profile flattens due to offshore transport of sediment from the beach and inner surf zone. Under calmer energy conditions, the profile steepens as sediment is transported onshore. Changes in energy conditions will generate changes in the direction of sediment transport and thereby also in the cross-shore profile. Typical morphological features appearing during beach recovery include intertidal bars and berms. The onshore movement of these morphological features appears fundamental to the overall processes of beach accretion and recovery (Hine, 1979; Thomas and Baba, 1986; Carter, 1988; Komar, 1998; Hughes and Turner, 1999).

Berms are accretional features, attributed to onshore sediment transport during swash, and they typically appear as sand or shingle bodies approximately parallel to the shoreline, and are characterized by an almost horizontal or slightly landward dipping top slope section (the berm top), and a more steeply seaward dipping section, which is the beach face (King, 1959; Hine, 1979; Okazaki, 1996; Hughes and Turner, 1999). The berm crest separates the two sections and it tends to be more distinct on coarse grained beaches than on fine grained beaches. The top level is typically located slightly above the mean high water mark or run-up limit, and the position of the berm is therefore normally determined by the mean high water tidal level.

Previous studies on the formation of berms have been mostly descriptive or qualitative (e.g. Duncan, 1964; King, 1959; Strahler, 1966; Hine, 1979; Thomas and Baba, 1986; Okazaki, 1996). Others have studied the relationship between wave height and berm elevation (Bagnold, 1940; Bascom, 1953; Okazaki, 1996; Sunamura, 1989). Sunamura (1989) observed that berm formation in the laboratory and in the field was controlled by the grain size (D_{50}) of the sediment, and that berms were formed on profiles composed of coarse sediment (D_{50} > ~0·69 mm) while bars were formed if the sediment was finer-grained. However, once formed, the berm height appears independent of grain size. Okazaki (1996) performed an extensive study on the relation between wave breaker type, wave height, grain size, standing waves and berm development, both in the laboratory and in the field. In Okazaki's (1996) experiments, berms were formed on profiles composed of sediment with grain sizes ranging from 0·22 to 5·2 mm. Furthermore, berm growth type and height were found to be dependent on grain size, because the grain size greatly influences the permeability and thereby the potential for the berm to stabilize. Both Sunamura's (1989) and Okazaki's (1996) work were performed on steep beach profiles ($\beta = 0{\cdot}1$).

Hine (1979) presented a detailed study of berm formation on a spit, where he identified three different mechanisms of berm development. The first mechanism, neap-berm development, is attributed to the development of a berm at the upper limit of the neap high-tide swash limit. The neap-berm is developed under fair-weather conditions and can be formed during the course of a few tidal cycles. As the tidal range increases with approaching spring tides, the neap-berm migrates onshore. If a pre-existing berm is present at a higher elevation on the beach, the neap-berm eventually welds to the existing berm which may continue to grow vertically and horizontally if swash overtopping occurs. The second mechanism, ridge-and-runnel development, is somewhat similar to the processes during neap-berm development. However, in this case, the berm formation is attributed to landward migration of an intertidal swash bar welding on to the beach face. This commonly occurs during post-storm conditions when sand previously transported offshore returns to the beach. As the swash bar begins to weld onto the beach face, the migration rate slows and the bar height decreases. Hydrodynamic and sediment transport processes in the mid-swash zone subsequently flatten the swash bar, which then is transformed into a beach face terrace. A new steeper beach face is established seaward of the former beach face and a new berm morphology is created further landward as a result of the flattened profile. The third mechanism, berm-ridge development, is attributed to a swash bar which has the top level at the spring high water elevation. At neap tides the swash bar is not overtopped and the gentle seaward slope acts as the beach face. Under mild wave conditions, the profile will adjust toward the equilibrium profile and thereby steepen. Thus, a new beach face is formed at the seaward margin of the swash bar.

Hine (1979) used the terms neap-berm, ridge-and-runnel, intertidal swash bars and swash bars. However, the terminology about berms, ridge-and-runnel, intertidal bars and swash bars have been rather inconsistent during time (King and Williams, 1949; King, 1959; Orford and Wright, 1978; Orme and Orme, 1988; Komar, 1998; Masselink *et al*., 2006). In the present paper, berms are defined as a ridge-like feature that has been, or is being, formed by swash processes, but which is spatially stable and with a steeper seaward than landward slope. An intertidal bar is a mobile ridge-like feature that has a steeper landward slope than seaward slope (slip-face bars) or is symmetric in shape (low-amplitude ridges). It may be affected by swash and/or surf zone processes. Swash bars are genetic terms and interpreted as intertidal bars and the term is therefore not used.

Despite recent extensive measurements of swash zone hydrodynamics and sediment transport in the field (Hughes *et al*., 1997; Butt *et al*., 2004; Hughes and Baldock, 2004; Masselink *et al*., 2005; Aagaard and Hughes, 2006; Hsu and Raubenheimer, 2006; Masselink and Russell, 2006; Hughes *et al*., 2007) only a limited number of field studies (e.g. Greenwood *et al*., 2004; Weir *et al*., 2006; Austin and Buscombe, 2008) have described the hydrodynamics during the formation of berms. Weir *et al*. (2006) documented two different modes of berm development on a steep, reflective beach (Avoca Beach, NSW, Australia). In Berm Growth Mode 1, an accumulation of sediment occurs on the upper beach face and berm crest, resulting in both vertical and horizontal growth of the berm. The net transport of sediment is landward, and the main sediment source is the inner surf and lower swash zones where swash interactions are prevalent. The onshore supply of sediment results in beach face steepening. The accretion/erosion boundary on the beach face is found to be most marked on the rising high tide when substantial swash overtopping occurs. This description of berm development agrees most closely with Hine's (1979) berm-ridge concept. In Berm Growth Mode 2, a net accumulation of sediment occurs on the mid to upper beach face, resulting in a horizontal progradation of the beach face, but no vertical growth of the pre-existing berm as swash overtopping does not occur. During the rising tide, the main sediment source is the lower swash zone where sediment is eroded and transported both landward and seaward. During the falling tide, sediment is eroded from the inner surf zone and transported landward to backfill the area eroded on the rising tide. The net result is a steepening of the beach face profile, but at a much slower pace than in Berm Growth Mode 1. This description of berm development agrees well with Hine's (1979) neap-berm concept. A main conclusion reached by Weir *et al*. (2006) was that the main factor determining which berm growth mode occurs is the presence or absence of swash overtopping of the pre-existing berm at the time of sediment accumulation on the beach face. The findings of Weir *et al*. (2006) on berm development are supported by observations on a steep gravel beach by Austin and Masselink (2006).

There are a number of studies describing intertidal bar dynamics in the upper part of the intertidal zone in relation to measured water level variations and wave heights (see review Masselink *et al*., 2006). However, very few field studies on berm formation with simultaneous measurements of water level and wave conditions. Those explicitly addressing berm formation have been undertaken on steep profiles composed of relatively coarse sediment, and with a dominance of motions at incident wave frequencies (e.g. Austin and Masselink, 2006; Weir *et al*., 2006). Consequently, further data is required for a wider range of beach type and wave conditions. The present paper addresses this issue and documents berm formation and development on a sandy, accreting and gently sloping beach which is significantly affected by infragravity wave motions. The morphological development is discussed with particular emphasis on the relationship between mean water levels (MWLs) and sediment transport rates. The paper is organized as follows: the next sections outline the field site, instrumentation and methodology. Results are presented in the fourth section, and include waves, wind and water levels,

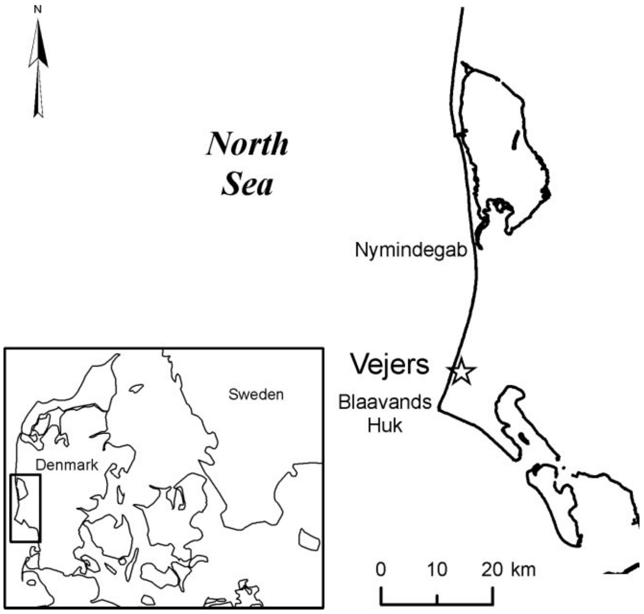

Figure 1. Sketch map showing the location of Vejers (marked with a star) on the west coast of Denmark.

morphological development and sediment transport rates derived from the profile measurements. The fifth section presents a discussion of the observations in terms of the concepts underlying Hine's (1979) model on berm development. Final conclusions follow in the last section.

Field Site

Vejers beach is located on the west coast of Denmark and is exposed to the North Sea (Figure 1). A cuspate foreland, Blaavands Huk, is located approximately 7 km further south. A shallow reef, Horns Rev, about 40 km long and 1–5 km wide, is attached to Blaavands Huk and extends in a westerly direction. In several places the water depth over the reef is less than 5 m. Thus, Blaavands Huk and Horns Rev work as a hydrographical barrier in such a way that the tidal range differs significantly to the north and south of the system. Tides at Vejers are semidiurnal, with spring and neap tidal ranges of approximately 1·2 and 0·6 m, respectively. The southerly directed net littoral drift is about $2{\cdot}3 \times 10^6$ $m^3 y^{-1}$ some 15 km north of Vejers and decreases to about zero at Blaavands Huk (KDI, 2001). This large gradient in the littoral drift facilitates the accretion (the rate of shoreline advance is about 1 m y^{-1}) that takes place at Vejers, where the subaerial beach is approximately 150 m wide and backed by 8–10 m high vegetated foredunes. The foreshore has a mean slope of $\beta \sim 0{\cdot}026$ and a mean grain size of 230 µm.

The mean annual offshore significant wave height (H_s) is 1·2 m and the maximum annual offshore wave height H_s is about 6·5 m. A multiple bar-system of 3–4 nearshore bars exists. At all times, waves tend to break by plunging across the seaward slopes of the bars and reform in the troughs. The beach state is modally intermediate (Wright and Short, 1984).

Methodology

Field experiments were conducted during the period 21 September–4 October 2007 along Line 6200, part of the Danish Coastal Authority's shoreline monitoring grid. A week prior to the experiments a storm event had flattened the intertidal profile and the field measurements therefore commenced during the initial phase of beach recovery. The profile was characterized by a high and flat berm (Berm 1) at about $x = 5$ m (Figure 2). To record morphological and sediment volume changes on the foreshore, twenty-seven 5 mm diameter steel rods with a spacing of 2 m were placed in a cross-shore transect. In order to estimate the net accretion or erosion across the transect, volumetric changes were recorded as m^3 per metre width of the beach under the assumption that elevation changes at each rod represented bed elevation changes within one square metre. For morphology with almost linear slopes this is a reasonable assumption. The rods were measured daily during low tide and every half hour over a full tidal cycle on certain days when wave conditions were expected to lead to significant profile adjustment. All rod measurements were referenced to a benchmark (DNN, the Danish Ordnance Datum, approximately corresponding to mean sea level) in the dunes using a Nikon Total Station. Additionally, a cross-shore profile along Line 6200, extending from the dunes to the upper shoreface, was collected once daily using the Nikon Total Station.

To record hydrodynamic parameters, four instrument stations were deployed. The stations consisted of a stainless steel H-frame equipped with various instruments. Only data from the pressure transducer mounted on Station 3 will be described in this study (Figure 2). The pressure transducer (Druck Model PTX1830, piezoelectric strain gauge transducer) was deployed a couple of centimetres below bed level in order to measure local wave heights and sea surface elevations. The sampling frequency was 16 Hz and the duration of each record was 34 min. Pressure sensors were calibrated in a stilling well at the field site and pressure records were detrended prior to computing wave heights. Mean water depths and water levels were determined through repeated surveys of instrument positions

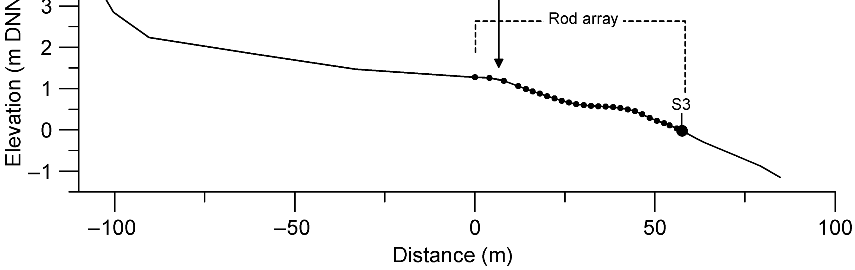

Figure 2. Surveyed cross-shore profile (22 September) and the location of the high berm (Berm 1), bed elevation rod array and instrument Station 3 (S3). DNN is Danish Ordnance Datum.

DOI: 10.1002/esp

and measurements of sensor elevations relative to the bed. Visual observations of wave breaker type and additional information on the beach state were noted for every instrument record. Wind conditions were observed as well using a handhold anemometer.

Inter-swash changes in the bed elevation were measured on a wave-by-wave basis using the method developed by Baldock *et al.* (2005) and further discussed by Brocchini and Baldock (2008). The method uses pressure transducers buried 5–10 cm below the sand surface in the swash zone. As the flow depth falls to zero, the signal recorded by the transducer is equal to the elevation of the water table and hence the elevation of the sand above the transducer, provided that the sand is close to fully saturated at that time. Immediately after the backwash on a medium to fine sand beach this is usually the case. An algorithm extracts the bed elevation and swash depths from the measured record. However, it should be noted that the technique relies on the water depth reducing to zero at the measurement location. Consequently, manual rod measurements are still required around the inner surf-swash zone boundary. For this field experiment, a cross-shore array of nine INW PT2X self-logging pressure transducers was deployed across the inner surf zone and swash zone. Each transducer was buried approximately 0·5 m north of one of the bed elevation rods to form a rod-transducer pair at the same cross-shore location. The pressure sensors were synchronized and logged at 4 Hz during each rod measurement period.

Data on atmospheric pressure, air temperature and wind direction were obtained from a weather station near the lighthouse at Blaavands Huk. Data were available every 10 minutes. Data on offshore significant and maximum wave heights H_s and H_{max}, wave periods T and wave directions were obtained from a Waverider buoy approximately 20 km north of Vejers. Data on water levels were obtained from a tide gauge station approximately 40 km north of Vejers, as well as at the inshore pressure sensor.

Results

Waves, wind and water level

Except for the first few days of the field campaign, the wind was mainly moderate and from northwest–northeast (Figure 3). The largest offshore waves (H_s about 2·75 m) occurred on the night between 21 and 22 of September. The smallest waves (H_s about 0·4 m) occurred on 3 October. Waves were mainly wind waves with periods of 4·5 seconds on average. The lowest wave periods ranged from 3·0 to 3·7 seconds. The largest wave periods, about 6·5 seconds, were observed on 26–27 September, when swell conditions occurred. The field campaign was conducted through a neap-spring-neap tidal cycle with spring tide occurring around 28–29 September. However, at the field site, the spring tide high water level was very low in comparison to the expected astronomical tide (Figure 3). This appears to be the result of a combination of high atmospheric pressure and strong offshore wind conditions.

Morphological changes

During the field campaign, the profile steepened due to net accretion on the upper foreshore and net erosion of the lower foreshore (Figure 4). This morphological development agrees well with the concept of profile steepening when calmer energy conditions follow a period of high-energy conditions which previously flattened the profile. The beach accretion on the upper foreshore was caused by onshore sediment transport from the lower swash zone and inner surf zone (see Figures 8 and 9 later), but the quantity of eroded sediment on the lower foreshore did not match the amount deposited. This suggests that some of the eroded sediment was transported offshore, and/or that three-dimensional effects prevailed such that not all the sediment transported landward was permanently deposited in this particular profile.

Foreshore development

In the present study, the foreshore is divided into the upper foreshore and the lower foreshore. The boundary between the lower and upper foreshore is defined as the level of the mean high water level, which during the field campaign was about 1 m. The upper foreshore is only affected by swash processes while the lower foreshore is affected by both surf zone processes, like propagating bores, and swash processes.

During the field campaign the morphological development of the lower foreshore was characterized by the formation of two berms that developed over two distinct periods, 22–24 September and 2 October–onwards, separated by a period with no berm present and only small morphological change. Comparing the two berm development events with the water levels and the astronomical tide shows that berm development occurred during periods with relatively low water levels (Figure 3). With rising water levels (between 24–25 September), the berm disappeared as surf conditions prevailed on the lower foreshore and the swash zone was translated to the upper foreshore.

At the following spring tide (28–29 September), water levels were very low. This was due to the passage of a high-pressure system and strong offshore winds from the northeast (Figure 3). The berm did not reform on the lower foreshore during this period despite the low water levels. It thus appears that a critical lower MWL exists for berm formation on gently sloping beaches. This critical limit is defined by the top level of the inner bar. If the water level drops to, or below this level, the wave energy level for berm development on the lower beach becomes too low due to the sheltering effect of the bar (Figure 4). The second berm development (2 October–onwards) will not be discussed further as field measurements during this period were sparse and the experiment stopped.

Figure 5 presents the daily rod profiles for the period 22 September–1 October 1 and shows the first berm building sequence that occurred on 22–24 September during the neap tide. The berm growth occurred through the onshore migration of a low intertidal bar (crest initially at about x = 40 m on the 22 September) which evolved to form a much higher berm with a crest at about x = 35 m on 23–24 September. While horizontally stabilized on 23 September vertical growth continued over 23–24 September. The maximum observed berm height was 0·4 m (berm crest to berm toe), and the berm had a gentle landward slope and steeper seaward slope. On 25 September, during rising MWLs (Figure 3), the berm flattened and the sediment was redistributed both onshore and offshore. During 25–28 September, during falling MWL, the sediment that had been transported offshore (to approximately x = 55 m), when the berm was flattened, was again transported onshore. This transport occurred as the migration of an intertidal bar that welded on to the foreshore and resulted in accretion on the upper foreshore (x = 10–30 m). During 28 September–1 October, with rapidly rising MWLs, erosion occurred over a large part of the lower foreshore profile and sediment was transferred to the upper foreshore where Berm 1 aggraded.

DOI: 10.1002/esp

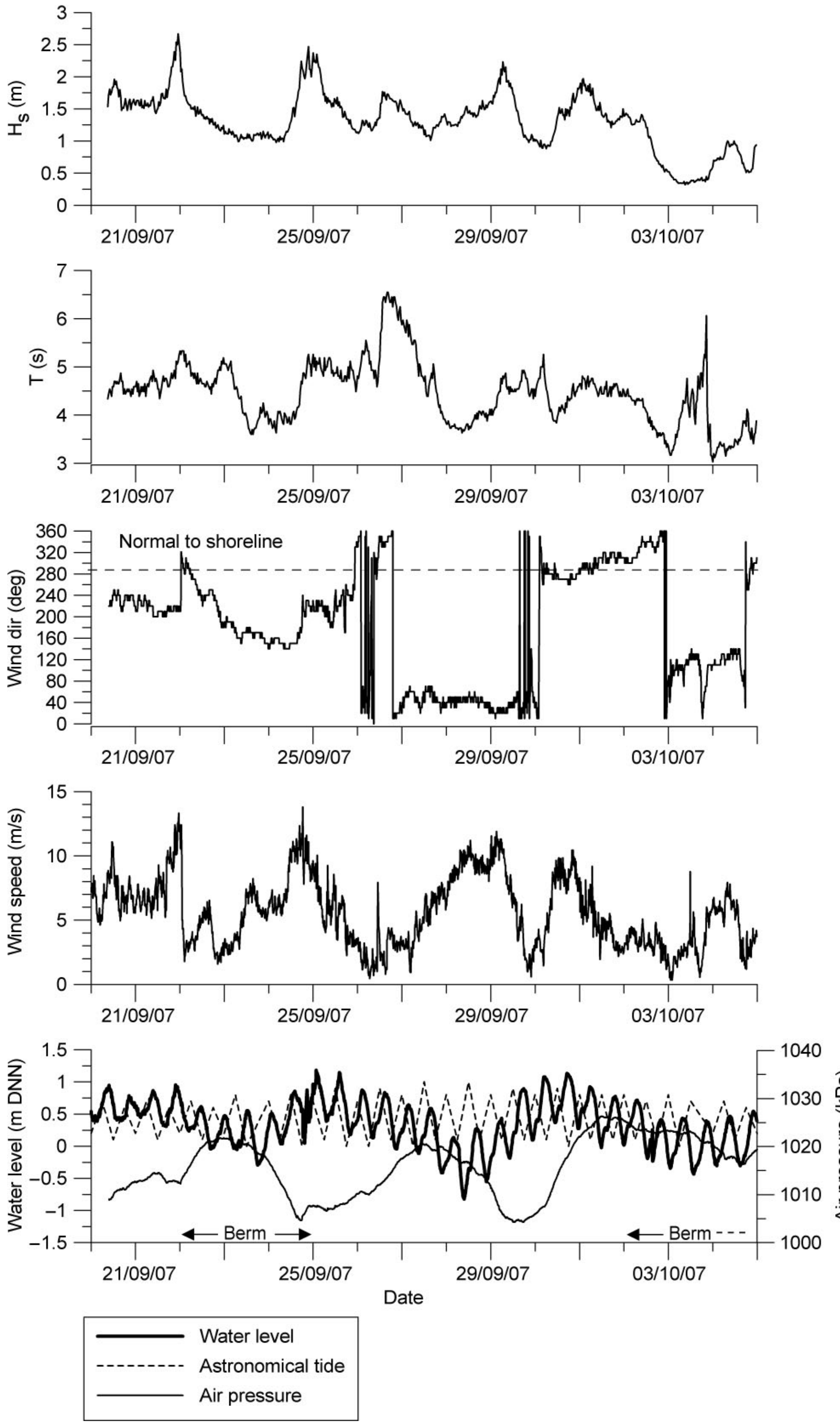

Figure 3. Summary of the offshore hydrodynamic conditions during the field campaign. From upper panel and down: Offshore significant wave height (H_s), wave periods (T), wind direction (degrees), wind speed and water levels (in metres). The lower panel illustrates measured and astronomically predicted water levels as well as atmospheric pressure. Berm occurrence is marked on the lowest time scale axis.

Figure 6 illustrates greater detail of the beach profiles on the upper foreshore for the period 22 September–2 October, and shows a continuous build-up of the pre-existing high berm (Berm 1; crest at about x = 5 m) with rising MWLs during 22–26 September. During 26–28 September, with falling MWLs, the runnel shoreward of the berm was filled in, and accretion also occurred on the seaward side of the berm, resulting in an overall flattening of the profile. Accretion occurred again during 28 September–2 October with rising water levels on 30–31 September. This continual development of the high berm indicates that onshore directed sediment transport occurred on the upper foreshore at high water levels.

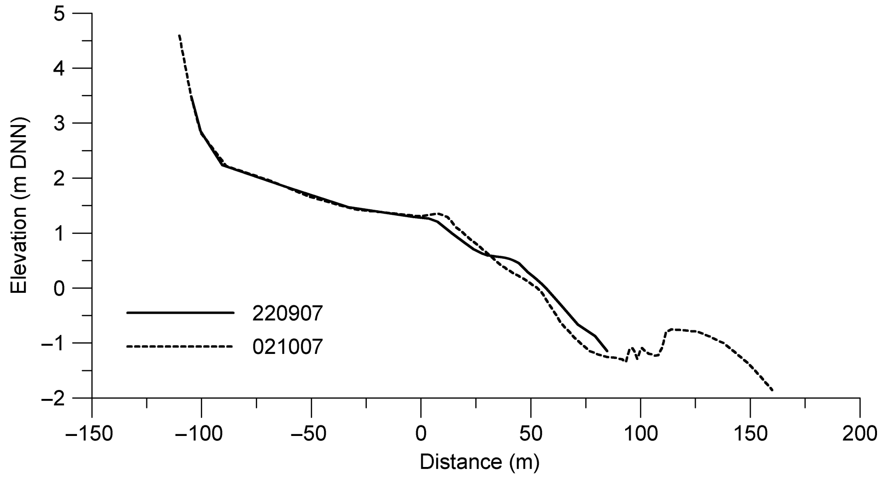

Figure 4. Net cross-shore profile change from the start to the end of the field campaign (22 September–2 October 2007).

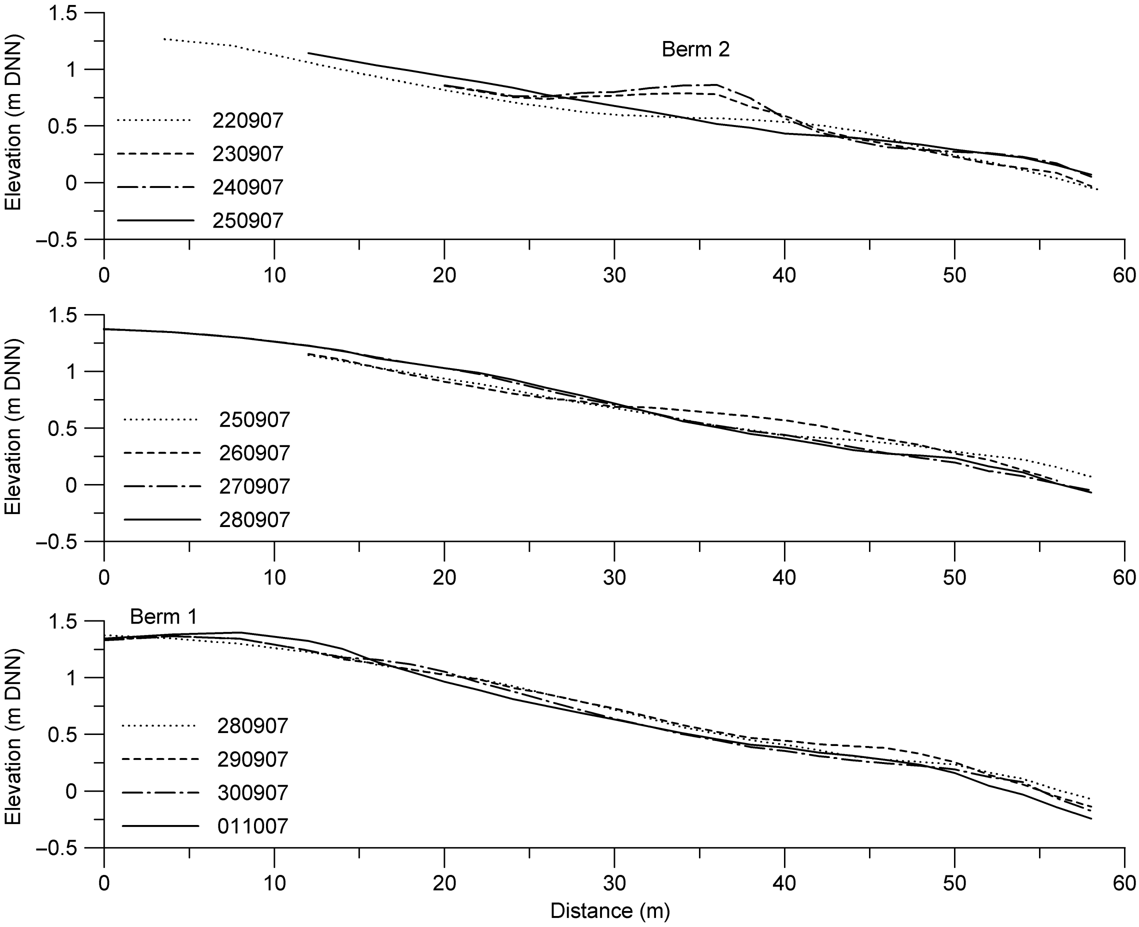

Figure 5. Daily profile changes from 22 September to 1 October 2007 and the location of Berms 1 and 2.

Foreshore processes

As described earlier, different morphological evolution of the foreshore was observed over different periods during the field experiments. On 24 September, when morphological changes were large, the foreshore development was characterized by a berm building sequence as an intertidal bar formed, grew, and moved onshore on the rising tide and finally merged with Berm 2 (Figure 7). The intertidal bar initially formed on the lower foreshore, at about $x = 55$ m, and welded on to Berm 2, where the berm crest was located at about $x = 35$ m. At high tide, Berm 2 translated further onshore as a new intertidal bar and filled in the runnel at about $x = 25$ m. The intertidal bar stabilized on the falling tide at about 14:30, with the resulting morphology characterized by a berm (Berm 3) at the location of the earlier runnel (crest at about $x = 23$ m). This intertidal bar and berm development is distinguished on the basis of the nomenclature outlined earlier, where a berm is defined as ridge-like feature that has been or is being formed by swash processes, but is spatially stable and with seaward slope asymmetry. An intertidal bar is a mobile ridge-like feature that has a landward slope asymmetry, or is symmetric in shape. It may be affected by swash and/or surf zone processes.

Examining the detailed bed level changes during 24 September (Figures 8a and 8b), a clear correlation between accretion in the upper swash and erosion in the lower swash

DOI: 10.1002/esp

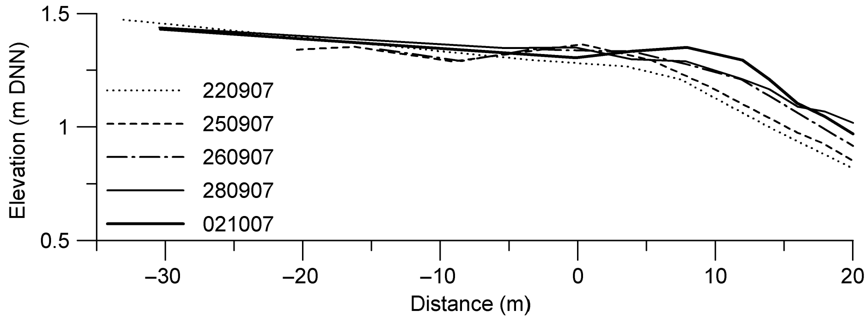

Figure 6. Cross-shore profile changes on the upper foreshore resulting in the build-up of the high berm (Berm 1).

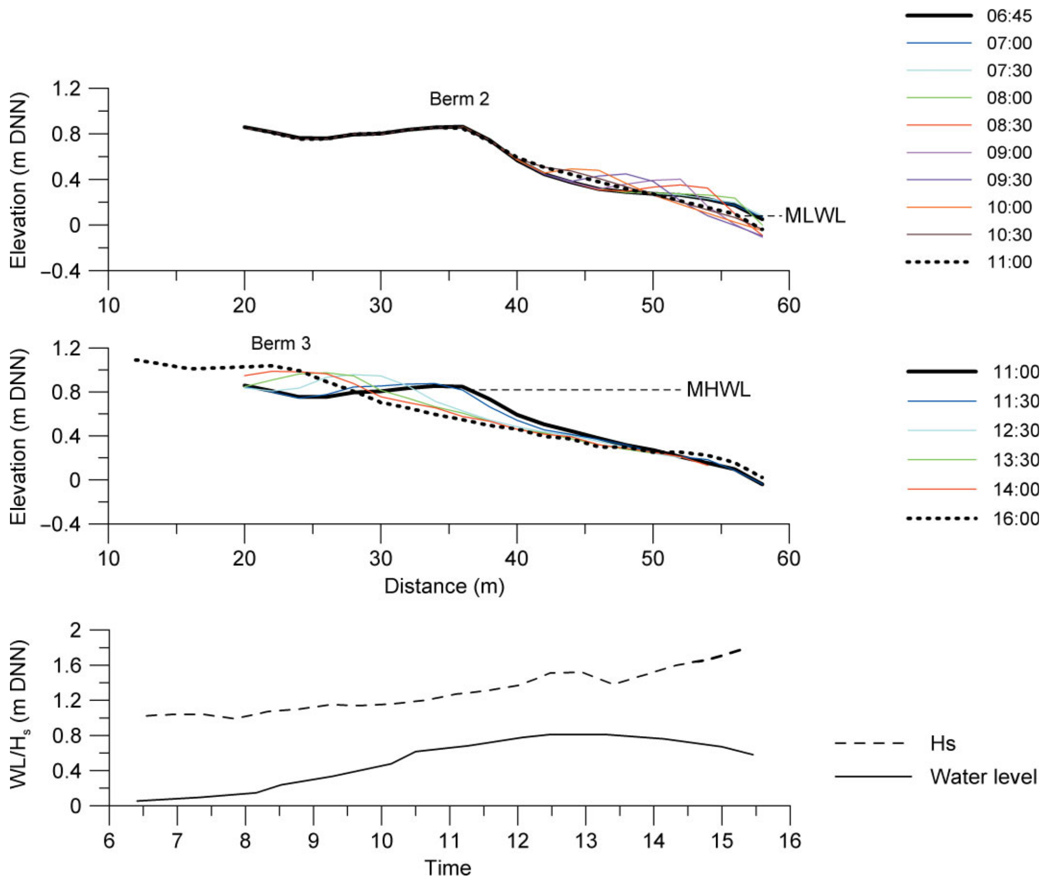

Figure 7. Profile changes on the lower foreshore, significant wave heights and the local water depth recorded at Station 3 on the rising and falling tide during 24 September. MLWL is the mean low water level (time 06:45) and MHWL the mean high water level (time 13:00). This figure is available in colour online at www.interscience.wiley.com/journal/espl

is observed during swash zone translation over the foreshore on the rising tide. During this period, the MWL was consistently just seaward of the crest of the intertidal bar. As a result of swash overtopping and sediment overwash, the beach is effectively truncated at the bar crest, the overtopping flow volume exits via the runnel and an incised lateral channel, and the net transport is usually predominantly shoreward (Aagaard *et al.*, 1998; Baldock *et al.*, 2005; Masselink *et al.*, 2008). This indicates that swash overtopping was the main factor controlling the intertidal bar migration. Between 10:00 and 10:30, the MWL moved seaward of the intertidal bar crest and the rate of morphological change immediately reduced. At about 10:30–11:00, as the intertidal bar merged with Berm 2, the rate of morphological change reduced further and became more uniform over the foreshore, and no clear correlation between accretion in the upper swash and erosion in the lower swash was observed. During this period, the active swash zone was the seaward face of Berm 2 and the slope on the upper foreshore was relatively steep, and the MWL was too low for significant swash overtopping to occur. Consequently, the backwash flow intensified in comparison to the earlier period, resulting in erosion of the upper foreshore and accretion on the lower foreshore where the eroded material was deposited. At about 11:00–11:30, the MWL level was sufficiently high for swash overtopping to re-occur, this time over Berm 2, rapid morphological change again occurred and the correlation between accretion in the upper swash and erosion in the lower swash was repeated. Berm 2 subsequently began to migrate onshore as a new intertidal bar. This sediment transport pattern continued until about 13:30 (Figure 8b) when overtopping largely ceased on the falling tide and the correlation between accretion in the upper swash and erosion in the lower swash also reduced. However, there is also a feedback process between the morphology and the effectiveness of

DOI: 10.1002/esp

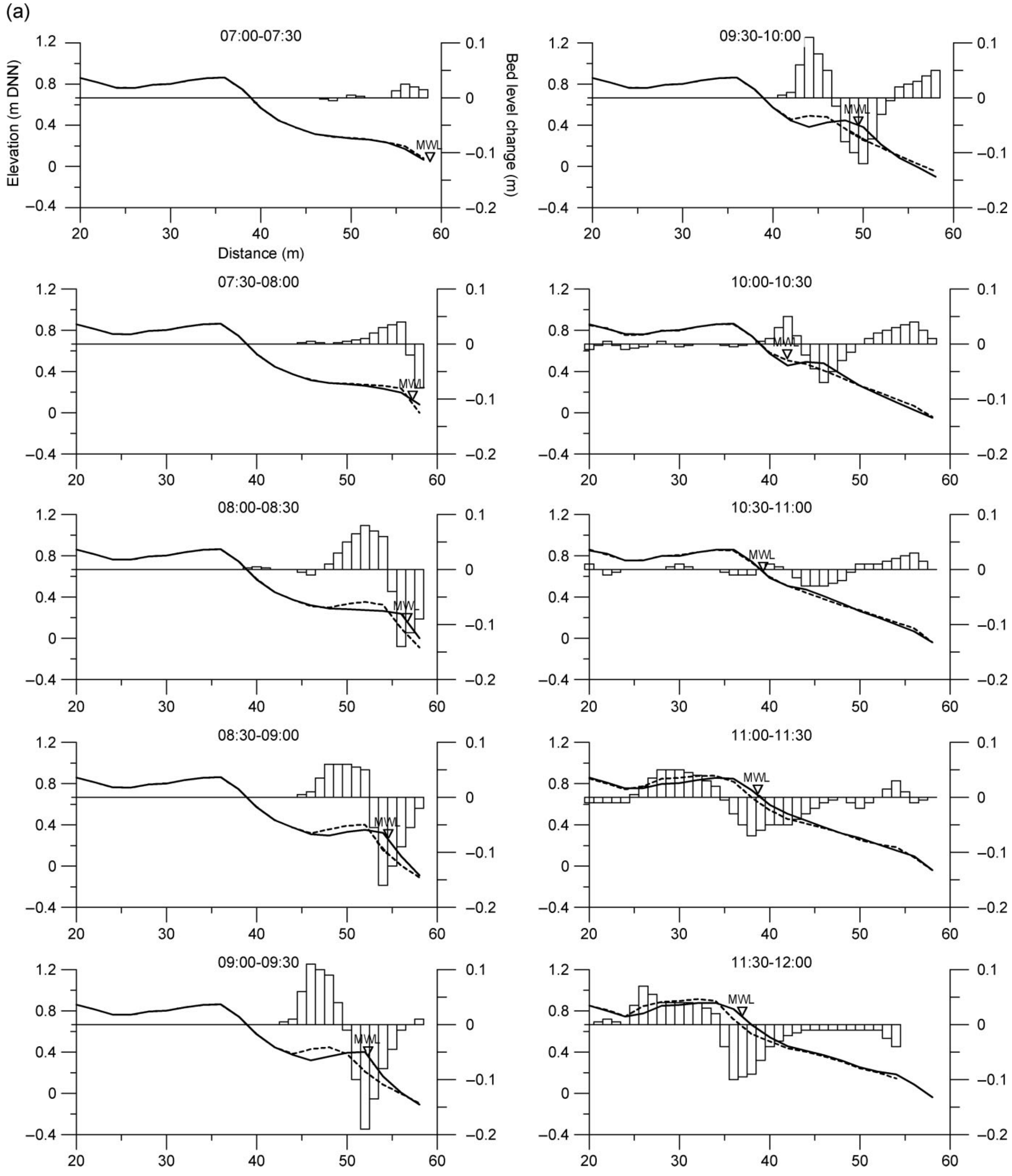

Figure 8. (a) Bed level changes (bars) determined from the bed elevation rods on the rising tide from 07:00–12:00 on 24 September. Solid line: start profile. Dotted line: end profile. MWL is the mean water level. (b) Bed level changes (bars) determined from the bed elevation rods from 12:00–16:00 on 24 September from high tide and during the falling tide. The tide began to fall at about 12:30. Solid line: start profile. Dotted line: end profile. MWL is the mean water level.

the overtopping process in driving net shoreward sediment transport. This is evident between 13:30 and 14:00, when the runnel seaward of Berm 2 became largely filled in. Consequently, although run-up still reaches a similar elevation on the beach face, the backwash is no longer reduced by the presence of the berm crest further seaward. The strong net shoreward transport therefore ceases. Between 13:30 and 15:00, the pattern of morphological change on the shoreface alternates between accretion and erosion as the effectiveness of the overtopping process decreases and increases as the relative position of the berm crest and MWL change in conjunction with gradual reshaping of the berm crest and runnel. After 15:00, almost no overtopping and overwash occurred and morphological changes became very small and more uniform across the profile. Furthermore, at about noon the wave heights began to increase (Figure 7) and the energy level, and thus the amount of water

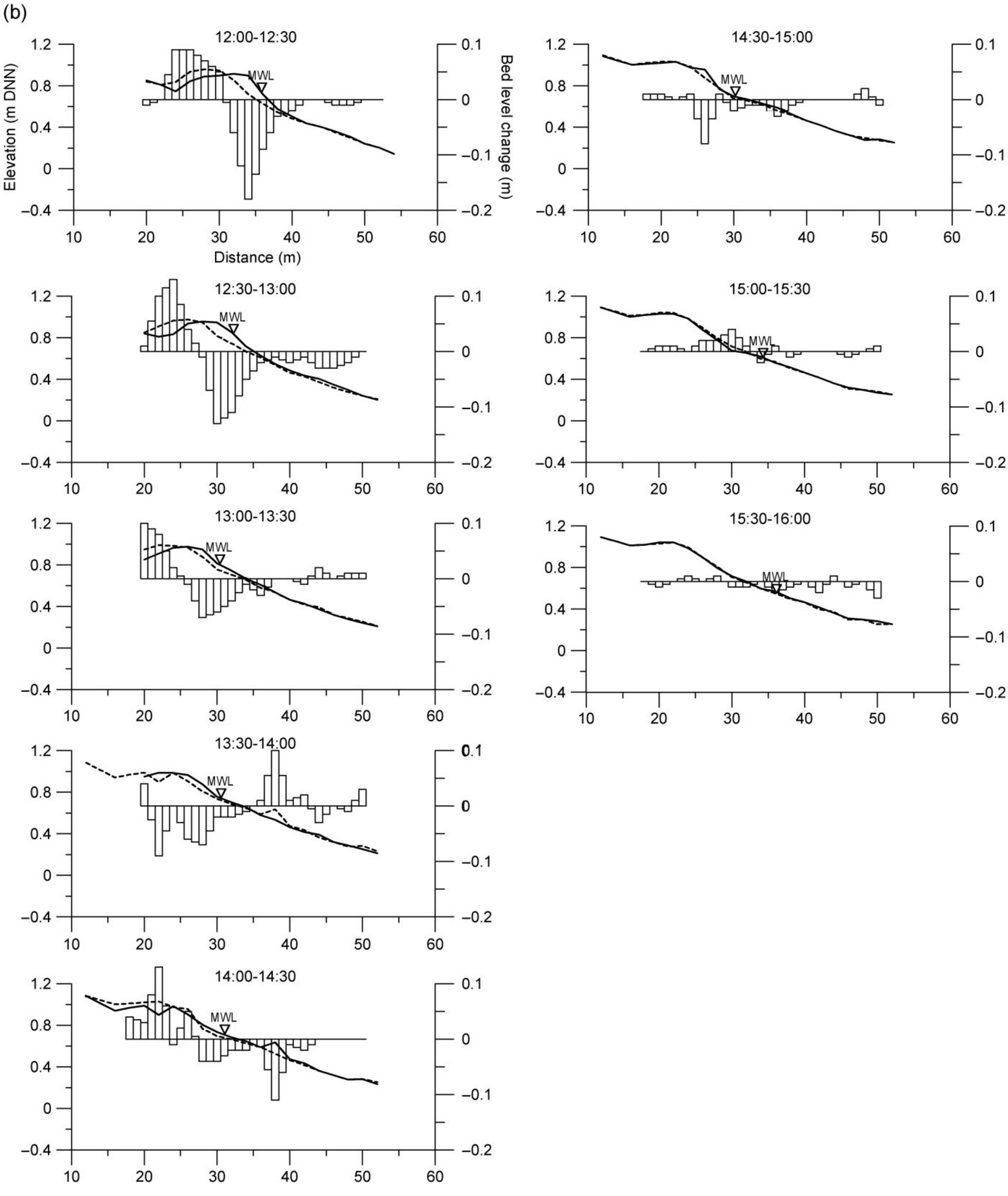

Figure 8. (*Continued*)

on the foreshore, increased during the falling tide. Because the drainage capacity of the runnel had decreased, as it was largely filled in, and the amount of water on the foreshore increased, due to increasing wave heights, the relative drainage effect of the runnel ceased. Thus, backwash flows became relatively larger reducing the net shoreward transport.

Inter-swash changes in the bed elevation is illustrated in Figure 9 which displays a comparison between the rod readings and the pressure transducers derived bed elevation for one rod-transducer pair. The accuracy of the rod readings is about 5 mm and the exact time of rod measurement is also uncertain (the rod array was measured every 30 minutes, taking 2–3 minutes to cover the array depending on wave and water level conditions). The automatic pressure sensor readings and the rod readings are the same within the measurement accuracy. While the drop in bed elevation recorded by the rod readings at $t \approx 90$–120 minutes is very significant and rapid, the rod measurements still under-estimate the rate of bed level change because of the low sampling rate. In particular, there are two very rapid reductions in bed elevation at 112 minutes and 116 minutes. The time-series of wave-by-wave measurements corresponding to these changes are illustrated

DOI: 10.1002/esp

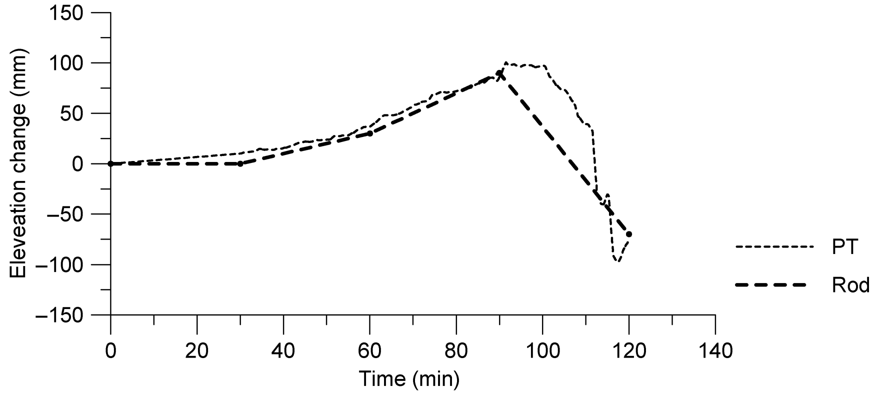

Figure 9. Bed elevation changes on 24 September, comparing measurements from ROD 18 and its paired pressure transducer (TB2).

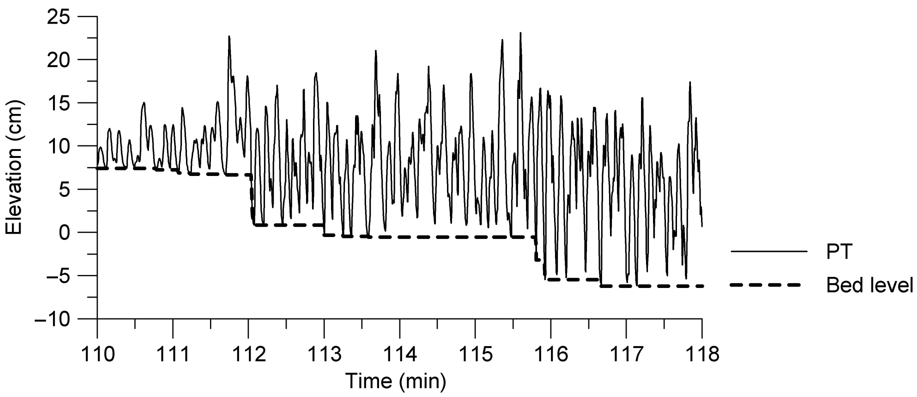

Figure 10. Bed elevation changes and water level from pressure transducer TB2, showing rapid reductions in bed elevation at 112 minutes and 116 minutes on 24 September.

in Figure 10. This illustrates bed level changes of order 5 cm over a few waves, and this is a result of the steep seaward face of the migrating berm translating shoreward past the measurement location. Note also the sudden increase in variance in the water surface elevation data at 112 minutes, which is consistent with a sudden reduction in the bed level allowing larger waves to penetrate to the measurement position.

Sediment transport

Cross-shore net sediment transport rates (Q) on 24 September were calculated for each measurement sequence by spatially differentiating the bed level changes from the first rod on the uppermost part of the profile to each succeeding rod further seaward and then converting sediment transport volumes to kg m^{-1} s^{-1} (Figure 11). The rates were determined from the sediment continuity equation:

$$Q(x_n) = Q(x_{n-1}) - \int_{x_{n-1}}^{x_n} \frac{\Delta Z_b}{\Delta t} dx \tag{1}$$

where ΔZ_b is the change in bed elevation over time interval Δt. For a quantitative application, the implicit assumption with this method is that no cross-shore variation in the gradient of the longshore transport exists. However, even if such exist, the model can be applied in a qualitative sense to evaluate erosion/accretion patterns, because $dQx/dx >> dQy/dx$. This procedure is useful in order to determine the magnitude and direction of the net sediment transport at each reference point in the profile, and it indicates the source of the transported sediment. On the rising tide, from 07:30–13:30, a very distinct and shoreward propagating erosion/accretion couplet formed as the swash zone translated across the foreshore. During this period, the position of the divergence of sediment transport from onshore to offshore occurred in the lower swash zone. This indicates that the migration of the first and second intertidal bars were due to internal reorganization of sediment within the foreshore zone. From 10:00–11:00, when the first intertidal bar merged with Berm 2, the erosion/accretion couplet was less distinct and the net sediment transport was mainly offshore-directed in the upper swash. The magnitude of this offshore directed sediment transport decreased in the lower swash zone. This is consistent with the conclusion earlier that the offshore directed transport in the upper swash at this time was due to the steep slope of Berm 2 and the low water level preventing swash overtopping and therefore onshore sediment transport. As the swash zone translated further onshore on the rising tide, the erosion/accretion couplet reappeared, with the shoreward transport reaching a maximum between 12:00 and 13:00, the top of the tide. At 13:30, when the water level began to fall and the wave heights increased, the net transport switched to offshore and the shape of the erosion/accretion couplet became less distinct. Subsequently, no strong pattern was observed in the transport magnitude and direction within the swash zone, and the direction of sediment transport shifted more or less randomly between onshore and offshore.

Interestingly, even though berms are classified as accretional features, the berm building sequence on 24 September did not result in a net sediment gain in the surveyed foreshore profile, but in fact a net loss. A possible explanation for this net loss is that on sandy beaches with low water infiltration

DOI: 10.1002/esp

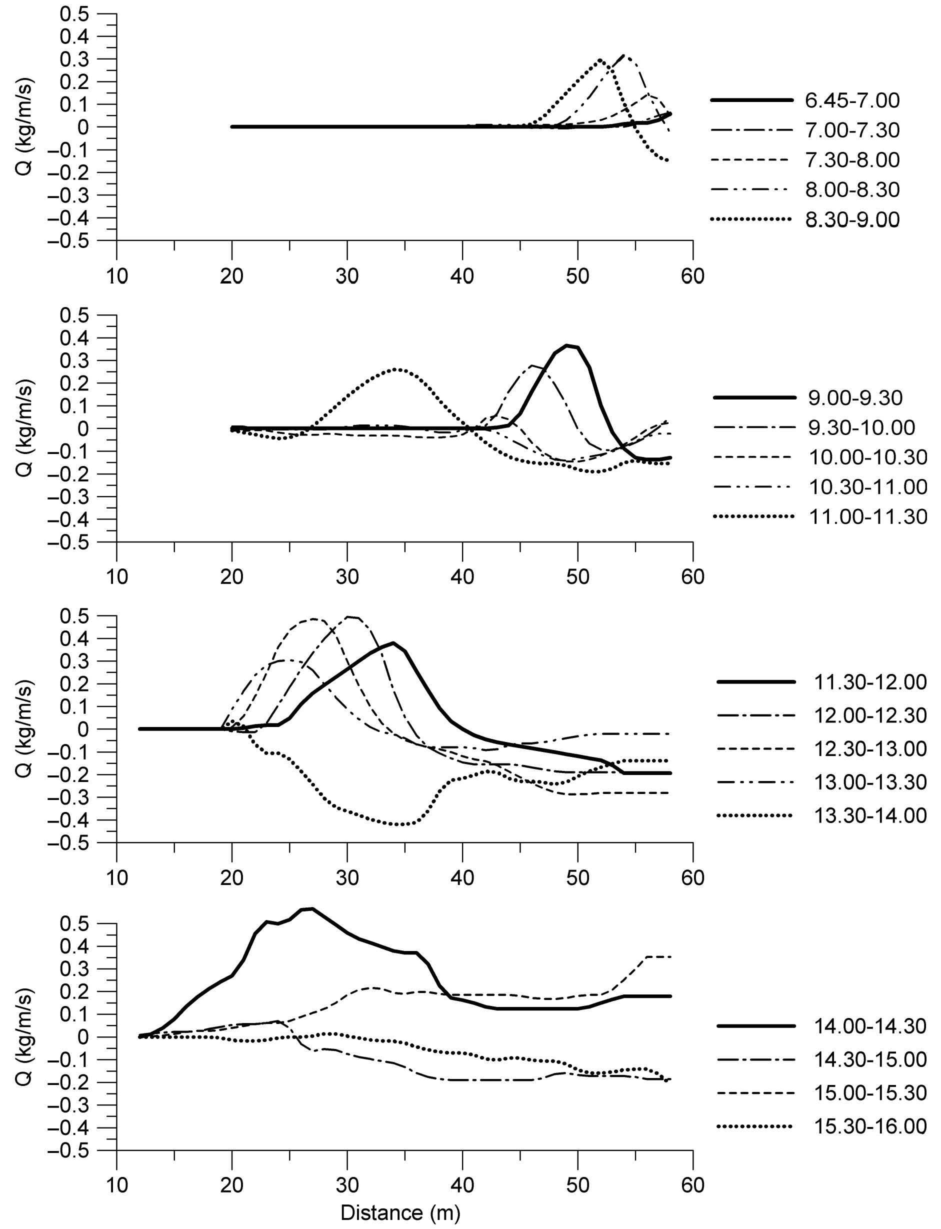

Figure 11. Cross-shore sediment transport rates (*Q*) across the foreshore profile during the rising and falling tide on 24 September. Rates are inferred from the spatial derivative of bed level change. Positive values represent onshore directed transport and negative values are offshore directed transport.

rates, rip channels tend to dissect the intertidal bars and berms, draining the runnels shoreward of the bars. On 24 September, three-dimensional effects were observed visually on the foreshore as a rip formed across the intertidal bar and Berm 2 to the south of the surveyed profile (Figure 12). Consequently, part of the sediment transported onshore due to swash overtopping of the berm was probably transported laterally and then offshore by the rip circulation and thereby removed from the surveyed profile. Furthermore, the increased backwash flows, induced by the fill in of the runnel and the increase in wave heights, might have counterbalanced or exceeded the onshore flows and thereby prevented accretion to occur on the foreshore on the falling tide.

Discussion

This study has documented berm formation and development on a gentle sloping and accreting beach at Vejers, Denmark and it has highlighted some of the similarities and dissimilarities

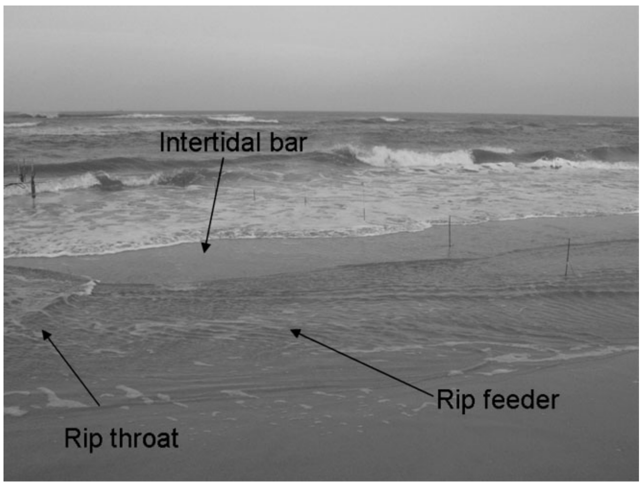

Figure 12. Photograph of the rip feeder in the runnel shoreward of the intertidal bar/Berm 2 on 24 September. The rip channel *per se* is at the extreme left of the photograph.

DOI: 10.1002/esp

between this beach and more steeply sloping, coarser-grained beaches. The observations on the onshore migration of intertidal bars and the formation of berms fit well with the concepts described in Hine's (1979) work. During 22–25 September, all three concepts were observed. However, differences were also observed and these are discussed here:

(i) According to Hine (1979), post-storm ridge-and-runnel development should be expected. Ridge-and-runnel development was observed in this field study, which was conducted post-storm. Initially, an intertidal bar migrated onshore on the upper foreshore, where it stabilized and transformed into a berm (Berm 2, Figure 5). However, the berm continued to grow while spatially stable, instead of decreasing in height, in contrast to Hine's (1979) description of ridge-and-runnel development. This was probably due to the occurrence of swash overtopping, consistent with the observations of Weir *et al.* (2006).

(ii) During the next tidal cycle, a new intertidal bar migrated onshore on the rising tide, and finally merged with the berm formed on the previous tide (Berm 2). This intertidal bar migration can be understood in the context of Hine's (1979) neap-berm concept, as the new intertidal bar was formed during neap-tide and the migration of the bar occurred through internal redistribution of the sediment, again because of overtopping.

(iii) As the tide continued to rise, the berm translated further onshore and finally merged with the high berm (Berm 1, Figure 6), which aggraded. This process was aided by a particularly high tide water level. Therefore, although not formed during spring tide, this berm development can be classified through Hine's (1979) berm-ridge concept which is expected to occur at the spring high water tide.

As pointed out by Hine (1979), berm development on the upper foreshore will lead to a profile steepening during the adjustment toward an equilibrium profile. Profile steepening did also occur in this field experiment, succeeding the berm building sequence, when no intertidal bars were observed. During this period the berm-ridge developed further, which again facilitated further profile steepening.

Hine (1979) defines the berm development concepts in the context of spring–neap cycles. However, this study shows that berm formation is strongly dependent on MWLs within the tidal cycle, and these are also affected by wind speed and direction and air pressure. This relationship becomes increasingly important on gently sloping beaches, as a change in water level greatly affects the water level translation rate which is more rapid than on steeply sloping beaches. Berm development on gently sloping beaches is probably therefore much more dynamic than on steeply sloping beaches.

The sediment transport during the migration of the intertidal bars on the rising tide was onshore directed in the upper swash and offshore directed in the lower swash, forming an erosion/accretion couplet. This is in agreement with the swash zone sediment transport shape function based on *in situ* measurements proposed by Aagaard and Hughes (2006). The couplet did not appear during the falling tide due to a lack of swash overtopping and hence accommodation space on the falling tide. The importance of the swash overtopping is further indicated by the small rates of sediment transport during the subsequent falling tide, which suggests that the profile was close to an equilibrium in the absence of overtopping. Apart from the lack of swash overtopping, the small rates of sediment transport on the falling tide might also have been caused by the fill in of the runnel and the increased wave heights on the falling tide, which may have caused the backwash flows to counterbalance the onshore flows. No significant erosion occurred on the foreshore profile despite the increased wave heights which supports the idea that the profile was close to an equilibrium under the wave conditions occurring on the falling tide.

The measurements on inter-swash bed level changes showed that large changes can occur during the excursion of only a few waves, and that the rod measurements underestimate the rate of bed level change because of the low sampling rate. These observations show that both rod measurements and higher frequency inter-swash bed level measurements are essential to provide the full details of the evolving bed morphology in the inner surf and swash zones.

The berm development observed in the present study differs from previous observations on steep beaches since several berm development stages occurred during a short period of time. As a result of the gentle slope of the beach face, the swash zone translated over a much wider cross-shore distance than on steep beaches, and hence intertidal bars and berms can become very dynamic features, exhibiting a range of responses to the dynamic boundary conditions. Furthermore, this field study was conducted on a sandy beach with low infiltration rate. On coarser-sediment steep beaches, higher infiltration rates are expected. This might cause intertidal bars to stabilize much faster, facilitating berm formation, which therefore is less dependent on changes in water level. Here, the intertidal bars were therefore very mobile, and berm formation highly dependent on the water level. For example, swash overtopping of the berm initiated intertidal bar migration in the present field study, while swash overtopping was the primary factor for berm growth with no migration in the study by Weir *et al.* (2006), which was conducted on a coarse-grained and steep beach with larger infiltration rates. This difference might be caused by differences in slope and infiltration rates.

In response to the berm accretion on the uppermost part of the foreshore the profile steepened during the field campaign. However, the volume of accretion on the foreshore did not match the erosion on the lower foreshore and upper shoreface, and overall beach accretion did not occur despite the onshore migration of (small) intertidal bars and the berm building. This was likely a result of an overall three-dimensional sediment transport pattern, where part of the sediment transferred landward through swash overtopping will be lost laterally along the runnels and then offshore through incised channels in the intertidal bars and berm. Therefore, in order for a beach to accrete significantly through cross-shore sediment transport mechanisms on short-time scales, these return flow mechanisms need to be weak or absent, which is probably more commonly the case on coarse-grained well-drained beaches. It is likely that accretion on gently sloping beaches like Vejers occurs in a more general sense on larger spatial and temporal scales through major bar-welding episodes following which the foreshore sediment reorganizes internally on shorter time scales through formation, migration and erosion of small intertidal bars and berms.

Conclusions

Berm formation and development was investigated on a gently sloping dissipative beach under low–moderate wave conditions. Berm formation occurred due to the onshore migration of intertidal bars, which stabilized as berms on the foreshore. On the rising tide and under rising water levels, the berms were transformed to intertidal bars, migrated further onshore and finally stabilized on the uppermost part of the foreshore, increasing the elevation of a pre-existing berm. The intertidal bar migration occurred on rising tides due to onshore directed

DOI: 10.1002/esp

sediment transport in the upper swash zone and offshore directed transport in the lower swash zone and thus an internal redistribution of sediment within the foreshore. The onshore directed transport in the upper swash was a direct result of swash overtopping and sediment overwash over the crest of the intertidal bar. Observations on large inter-swash bed level changes indicates that both rod measurements and higher frequency inter-swash bed level measurements are essential to provide the full details of the evolving bed morphology in the inner surf and swash zones.

The observed berm development stages agree with the concepts of neap-berm, ridge-and-runnel and berm-ridge development proposed by Hine (1979). However, the berm development was more dependent variations in the water level over the tidal cycle, and on wind and pressure-induced variations in tidal water levels, than on the spring–neap tidal cycles.

Intertidal bars and berms on gentle sloping beaches appear to be very dynamic features due to the rapid translation rate of the MWL during the tidal cycle. During the field campaign, all three concepts of berm development proposed by Hine (1979) were observed in the course of only three tidal cycles. The rapid development was due to the gentle beach slope and low infiltration rates. In contrast to berm development on the steep, well-drained and coarser-grained beach studied by Weir *et al.* (2006), the observed berms were very mobile due to substantial swash overtopping. However, despite the onshore migration of intertidal bars and the formation of new berms, beach accretion did not occur. This was most likely due to the development of lateral flow and sediment transport in the runnel shoreward of the intertidal bars and berm, which then returned seaward through a nearby rip channel in the bars.

Acknowledgements—This work was funded by the Danish Natural Sciences Research Council (FNU) through grant number 272-05-0415. Stine G. Jensen was funded by the Faculty of Science, University of Copenhagen through a PhD scholarship. We thank the Department of Forestry and Nature for permission to work at Vejers and for the loan of the mobile cabin. Bo Dalbjerg Jensen (University of Copenhagen) and Dave Mitchell (University of Sydney) assisted with the installation of the electronics. We are grateful to Per Sørensen (Danish Coastal Authority) for supplying the offshore wave records. Furthermore, we thank two anonymous reviewers for their comments on the current paper.

References

Aagaard T, Hughes M. 2006. Sediment suspension and turbulence in the swash zone of dissipative beaches. *Marine Geology* **228**: 117–135.

Aagaard T, Nielsen J, Nielsen N, Greenwood B. 1998. Suspended sediment transport and morphological evolution on an intertidal beach. In *Proceedings Coastal Dynamics '97*. ASCE: Plymouth; 824–833.

Austin MJ, Buscombe D. 2008. Morphological change and sediment dynamics of the beach step on a macrotidal gravel beach. *Marine Geology* **249**: 167–183.

Austin MJ, Masselink G. 2006. Observations of morphological change and sediment transport on a steep gravel beach. *Marine Geology* **229**: 59–77.

Bagnold RA. 1940. Beach formation by waves: some model experiments in a wave tank. *Journal Institution of Civil Engineers* **15**: 27–52.

Baldock TE, Hughes MG, Day K, Louys J. 2005. Swash overtopping and sediment overwash on a truncated beach. *Coastal Engineering* **52**(7): 633–645.

Baldock TE, Matthew PB, Michael GH. 2005. Field observations of instantaneous cross-shore free surface profiles and flow depths in the swash zone. In *Coastal Dynamics 2005*, Agustin S-A (ed.). ASCE: Barcelona.

Bascom WH. 1953. Characteristics of natural beaches. In *Proceedings of the 4th Coastal Engineering Conference*. ASCE: Reston, VA; 163–180.

Brocchini M, Baldock TE. 2008. Recent advances in modeling swash zone dynamics: influence of surf–swash interaction on nearshore hydrodynamics and morphodynamics. *Reviews of Geophysics* **46**: RG3003.

Butt T, Russell P. 2000. Hydrodynamics and cross-shore sediment transport in the swash-zone of natural beaches: a review. *Journal of Coastal Research* **16**(2): 255–268.

Butt T, Russell P, Puleo J, Miles J, Masselink G. 2004. The influence of bore turbulence on sediment transport in the swash and inner surf zones. *Continental Shelf Research* **24**(7–8): 757–771.

Carter RWG. 1988. *Coastal Environments. An Introduction to the Physical, Ecological and Cultural Systems of Coastlines*. Academic Press: London; 616 pp.

Duncan Jr JR. 1964. The effects of water table and tide cycle on swash-backwash sediment distribution and beach profile development. *Marine Geology* **2**: 186–197.

Greenwood B, Aagaard T, Nielsen J. 2004. Swash bar morphodynamics in the Danish Wadden Sea: sand bed oscillations and suspended sediment flux during an accretionary phase of the foreshore cycle. *Danish Journal of Geography* **104**(1): 15–30.

Hine AC. 1979. Mechanisms of berm development and resulting beach growth along a barrier spit complex. *Sedimentology* **26**: 333–351.

Hughes MG, Baldock TE. 2004. Eulerian flow velocities in the swash zone: field data and model predictions. *Journal of Geophysical Research-Oceans* **109**: C08009.

Hughes M, Turner I. 1999. The beach face. In *Handbook of Beach and Shoreface Morphodynamics*, Short AD (ed.). John Wiley & Sons: Chichester; 119–144.

Hughes MG, Aagaard T, Baldock TE. 2007. Suspended sediment in the swash zone: heuristic analysis of spatial and temporal variations in concentration. *Journal of Coastal Research* **23**(6): 1345–1354.

Hughes MG, Masselink G, Brander RW. 1997. Flow velocity and sediment transport in the swash zone of a steep beach. *Marine Geology* **138**: 91–103.

Hsu TJ, Raubenheimer B. 2006. A numerical and field study on inner-surf and swash sediment transport. *Continental Shelf Research* **26**(5): 589–598.

KDI. 2001. *The Sediment Budget Along the West Coast of Jutland*, Report. Danish Coastal Authority: Lemvig; 54 pp (in Danish).

King CAM. 1959. *Beaches and Coasts*. Edward Arnold: London; 403 pp.

King CAM, Williams WW. 1949. The formation and movement of sandbars by wave action. *Geographical Journal* **113**: 70–85.

Komar PD. 1998. *Beach Processes and Sedimentation*. Prentice Hall: Englewood Cliffs, NJ; 544 pp.

Masselink G, Hughes M. 1998. Field investigation of sediment transport in the swash zone. *Continental Shelf Research* **18**(10): 1179–1199.

Masselink G, Puleo JA. 2006. Swash-zone morphodynamics. *Continental Shelf Research* **26**(5): 661–680.

Masselink G, Russell P. 2006. Flow velocities, sediment transport and morphological change in the swash zone of two contrasting beaches. *Marine Geology* **227**(3–4): 227–240.

Masselink G, Kroon A, Davidson-Arnott RGD. 2006. Morphodynamics of intertidal bars in wave-dominated coastal settings – a review. *Geomorphology* **73**: 33–49.

Masselink G, Evans D, Hughes MG, Russell P. 2005. Suspended sediment transport in the swash zone of a dissipative beach. *Marine Geology* **216**(3): 169–189.

Masselink G, Austin MJ, Tinker JT, O'Hare T, Russel PR. 2008. Cross-shore sediment transport and morphological response on a macro-tidal beach with inter-tidal bar morphology, Truc Vert, France. *Marine Geology* **251**: 141–155.

Okazaki S. 1996. *A Study of Berms on Sandy Beaches*, science report. Geoscience, Univiversity of Tsukuba: Tsukuba; Section A, vol. 17, 60 pp.

Orford JD, Wright P. 1978. What's in a name? – Descriptive or genetic implications of 'ridge and runnel' topography. *Marine Geology* **28**: M1–M8.

Orme AR, Orme AJ. 1988. Ridge-and-runnel enigma. *Geographical Review* **78**: 169–184.

Pritchard D, Hogg AJ. 2005. On the transport of suspended sediment by a swash event on a plane beach. *Coastal Engineering* **52**: 1–23.

Puleo JA, Beach RA, Holman RA, Allen JS. 2000. Swash zone sediment suspension and transport and the importance of bore-generated turbulence. *Journal of Geophysical Research – Oceans* **105**(C7): 17021–17044.

Strahler AN. 1966. Tidal cycle of changes in an equilibrium beach, Sandy Hook, New Jersey. *Journal of Geology* **74**(3): 247–268.

Sunamura T. 1989. Sandy beach geomorphology elucidated by laboratory modeling. In *Applications in Coastal Modeling*, Lakhan VC, Trenhaile AS (eds). Elsevier: Amsterdam; 159–213.

Thomas KV, Baba M. 1986. Berm development on a monsoon-influenced microtidal beach. *Sedimentology* **33**: 537–546.

Weir FM, Hughes MG, Baldock TE. 2006. Beach face and berm morphodynamics fronting a coastal lagoon. *Geomorphology* **82**: 331–346.

Wright LD, Short AD. 1984. Morphodynamic variability of surf zones and beaches; a synthesis. *Marine Geology* **56**: 93–118.

DOI: 10.1002/esp